Geochemical Journal, Vol. 46, pp. 287 to 295, 2012

Depth profiles of radioactive cesium and iodine released from the Fukushima Daiichi nuclear power plant in different agricultural fields and forests

TAKESHI OHNO,[1]* YASUYUKI MURAMATSU,[1] YOSHINORI MIURA,[2] KAZUMASA ODA,[1] NAOYA INAGAWA,[1] HIROMU OGAWA,[1] ATSUKO YAMAZAKI,[1] CHIAKI TOYAMA[1] and MUTSUTO SATO[3]

[1]Department of Chemistry, Faculty of Science, Gakushuin University, Mejiro 1-5-1, Toshima-ku, Tokyo 171-8588, Japan
[2]Agriculture, Forestry and Fisheries Department, Fukushima Prefecture, Sugitsumacho, Fukushima, Fukushima 960-8670, Japan
[3]Fukushima Agricultural Technology Centre, Hiwada, Koriyama, Fukushima 963-0531, Japan

(*Received January 27, 2012; Accepted June 4, 2012*)

In order to understand the behavior of radionuclides released from the Fukushima Daiichi nuclear power plant, the depth distributions of radiocesium and radioiodine were investigated in a wheat field, a rice paddy, an orchard, and a cedar forest in Koriyama, Fukushima Prefecture. Our results demonstrate that, following the nuclear power plant disaster, more than 90% of the radionuclides were distributed in the upper 6 cm of the soil column in the wheat field and within 4 cm of the surface in the rice paddy, orchard, and cedar forest. According to the measurement of radionuclides in the three adjacent agricultural fields, the variation of deposition densities in the wheat field was smaller than that of the orchard and rice paddy, suggesting that the low permeability of the orchard and paddy soils may cause horizontal migration of radionuclides during the initial deposition. This result indicates that the deposition densities in the wheat field should be appropriate for estimating the amount of fallout in the area. The deposition densities of ^{134}Cs, ^{137}Cs, and ^{131}I in this area were estimated to be 512 ± 76 (SD, n = 5), 522 ± 80 (SD, n = 5), and 608 ± 79 (SD, n = 5) kBq/m^2 (decay corrected to April 1, 2011), respectively. A comparison of the deposition density between the wheat field and the cedar forest suggests that more than half of the radionuclides are distributed in the tree canopies of the evergreen forestland.

Keywords: Fukushima Daiichi nuclear power plant accident, ^{134}Cs, ^{137}Cs, ^{131}I, agricultural field

INTRODUCTION

The accident at the Fukushima Daiichi nuclear power plant resulted in a substantial input of radionuclides into the environment, including atmospheric releases of ^{134}Cs (half-life: 2.07 y), ^{137}Cs (30.1 y), and ^{131}I (8.02 d) (Chino *et al*., 2011). Most parts of eastern Japan were subjected to radioactive contamination and Fukushima Prefecture was most affected (MEXT, 2011; Kinoshita *et al*., 2011). Since agriculture is the main industry in Fukushima Prefecture, it is important to survey the distribution and behavior of radioactive substances in agricultural fields to assess their usage for plant cultivation, as well as for radiation safety for people living in the area. The risk of exposure for farmers and local populations as well as that of internal exposure for consumers from contaminated agricultural products is of public concern.

The migration of radiocesium and radioiodine from nuclear weapons fallout and from the Chernobyl accident has been studied extensively (e.g., Beck, 1966; Muramatsu *et al*., 1987; Bunzl *et al*., 1995; Orlov *et al*., 1996; Ivanov *et al*., 1997, Rosén *et al*., 1999; Almgren and Isaksson, 2006). These studies suggest that knowledge of the initial depth distribution of fallout radionuclides is important for future decontamination work and countermeasures to reduce the transfer of radionuclides to agricultural products. In order to determine how the initial depth distribution of the radioactive substances varies depending on field type, such as wheat fields, rice paddies, orchards, and forestland, we need to take measurements at locations with different land-use patterns but with nearly equal exposure to radioactive fallout. The Fukushima Agricultural Technology Centre has wheat fields, rice paddies, orchards, and forestland all enclosed within a 500 × 500 m test site. At this test site, we sampled and determined the depth profiles of radiocesium and radioiodine for each type of land use. On the basis of these depth profiles, we derived an estimate of the deposition density to clarify the influence that land use has on the distribution pattern of radionuclides in soils. Several other studies have been also conducted in this issue for the distribution of the radionuclides on land and mechanism of retention of radiocesium at soil surface (Watanabe *et al*., 2012; Qin *et al*., 2012).

*Corresponding author (e-mail: takeshi.ohno@gakushuin.ac.jp)

Materials and Methods

Sampling was carried out on April 23 and 24, 2011, at the Fukushima Agricultural Technology Centre, which is located 60 km west of the Fukushima Daiichi nuclear power plant. From 1981 to 2010, the mean annual precipitation in the area was 1163 mm and the mean annual temperature was 12.1°C (Kohriyama Weather Station, Japan Meteorological Agency). According to the airborne monitoring survey by the Ministry of Education, Culture, Sports, Science and Technology (MEXT), the deposition density or inventory of ^{134}Cs and ^{137}Cs in this area following the nuclear disaster was 300–600 kBq/m^2. This centre has three different types of agricultural fields and a cedar forest within a 25-ha study area where we were able to investigate the behavior of radionuclides in each field. In this study, we used a stainless core sampler (30 cm in length, 5 cm in diameter) to collect five samples with a random spatial distribution within a 100-m^2 (10 × 10 m) area of each field to estimate the statistical dispersion. Sampling of soil with uneven soil surfaces was avoided, since, if there were cracks, rainwater containing radionuclides would readily sink into the ground and the depth profile would be changed. The wheat field had been plowed following the harvest, and there was little grass at the time of sampling. The rice paddy had not been plowed following the harvest in the autumn, and we collected samples where there was no stubble. Sampling of the soil in the orchard was carried out in the intercanopy gaps. The soil surface of the orchard is usually covered with undergrowth. However, in order to eliminate the influence of filtration effects from grasses, we collected soil samples from places where there was little grass. Sampling of the soil in the forest was carried out under the canopy. In this case, we firstly gathered leaf litter by hand, and then collected soil samples using the core sampler. The soil types of the samples for the wheat field, orchard, rice paddy, and forest were gray lowland soil, brown forest soil, gray lowland soil, and brown forest soil, respectively.

The core samples were divided into 6 portions (0–2 cm, 2–4 cm, 4–6 cm, 6–10 cm, 10–15 cm, 15–20 cm) to examine the depth profiles of radiocesium and radioiodine. To prevent possible loss of iodine, the samples were not dried before the measurement of the radioactivity. The samples were mixed well without removing any rock fragments and then placed in plastic bottles (50 mm in diameter and 50 mm in height). After the measurement, the samples were dried at 100°C for 12 h and the weight of the dry soil was determined.

The concentrations of radionuclides in the samples were determined using a germanium semiconductor detector coupled to a multichannel analyzer (Canberra, Meriden, U.S.A.). Gamma-ray peaks used in the measurements were 604 keV for ^{134}Cs, 662 keV for ^{137}Cs, and 636 keV for ^{131}I. The counting time was 2000–60000 s. The decay was corrected to April 1, 2011, using the half-lives (i.e., decay constants) of the nuclides. Efficiency calibrations for the detector for the different geometries used in the measurement were performed using a mixed radionuclide reference standard (matrix: aluminum oxide) provided by the Japan Radioisotope Association. Standard reference materials such as IAEA372 (grass), IAEA375 (soil), and IAEA444 (soil) were analyzed to validate the analytical accuracy. Radiocesium was detected in all samples analyzed in this study, and counting errors for the measurements of ^{134}Cs and ^{137}Cs were usually less than 10%. In contrast, the radioactivity measurements for iodine were performed in June, and it was not detected in many samples owing to the short half-life of ^{131}I. Therefore, it should be noted that the attenuation of radioiodine could result in an underestimation in the amount local fallout.

Results and Discussion

The concentrations and depth distributions of ^{134}Cs, ^{137}Cs, and ^{131}I in the wheat field are shown in Table 1. Additionally, the activity contained in each depth portion was divided by the total activity of the core (0–20 cm), and these values are also shown in the table. The relative proportion of radiocesium situated within 2 cm of the surface varied from 50% to 86% of the whole-core inventory, while radioiodine varied from 42% to 70%. Although there was a good deal of variability, the relative proportion of radioiodine within 2 cm of the surface was smaller than that of radiocesium. This suggests that the movement of radioiodine is faster than that of radiocesium, which is consistent with previous studies (Tanaka *et al*., 2012; Kato *et al*., 2012). The results of these depth profiles reveal that more than 90% of the ^{134}Cs, ^{137}Cs, and ^{131}I were distributed within 6 cm and in many cases within 4 cm of the soil surface. In order to estimate the deposition density (kBq/m^2), total activities of the core samples were calculated by summing the radioactivity over the whole depth, and for ^{134}Cs, ^{137}Cs, and ^{131}I in the wheat field, the total activities were in the ranges 866–1200, 880–1230, and 1060–1440 Bq, respectively. According to the assumption that the radionuclides did not migrate horizontally, the deposition densities of ^{134}Cs, ^{137}Cs, and ^{131}I in the wheat field were estimated to be 512 ± 76 (SD, n = 5), 522 ± 80 (SD, n = 5), and 608 ± 79 (SD, n = 5) kBq/m^2 (decay corrected to April 1, 2011), respectively.

The concentrations of ^{134}Cs, ^{137}Cs, and ^{131}I for different soil profiles in the orchard are shown in Table 2. Because of the short half-life, the radioactivity of ^{131}I was not detected in many samples. The proportion of

Table 1. Depth distribution of ^{134}Cs, ^{137}Cs, and ^{131}I concentrations in the wheat field

	Depth (cm)	Weight (g)	Bulk density (g/cm^3)	^{134}Cs (Bq/kg dw)	Inventory (%)	^{137}Cs (Bq/kg dw)	Inventory (%)	^{131}I (Bq/kg dw)	Inventory (%)	^{134}Cs/^{137}Cs	^{131}I/^{137}Cs
H0	0–2	40	1.0	18700 ± 100	86	19200 ± 100	86	18500 ± 400	70	0.97	0.96
	2–4	40	1.0	2200 ± 30	10	2220 ± 50	10	6100 ± 210	23	0.99	2.75
	4–6	51	1.3	468 ± 15	3	486 ± 22	3	1120 ± 90	5	0.96	2.30
	6–10	100	1.3	66.0 ± 2.4	1	73.6 ± 3.4	1	117 ± 15	1	0.90	1.59
	10–15	135	1.4	8.9 ± 1.2	0	11.6 ± 1.9	0	ND		0.76	
	15–20	137	1.4	3.0 ± 0.5	0	7.8 ± 0.7	0	ND		0.38	
	Deposition density (kBq/m^2)			448		459		541			
H1	0–2	52	1.3	11500 ± 100	53	11700 ± 100	53	13600 ± 400	49	0.98	1.16
	2–4	50	1.3	6690 ± 50	30	6810 ± 80	30	9850 ± 330	34	0.98	1.45
	4–6	48	1.2	2110 ± 20	9	2120 ± 30	9	3390 ± 150	11	1.00	1.60
	6–10	82	1.1	760 ± 7	6	813 ± 11	6	735 ± 47	4	0.93	0.90
	10–15	143	1.5	183 ± 3	2	199 ± 5	2	ND		0.92	
	15–20	137	1.4	43.8 ± 0.8	1	52.0 ± 1.1	1	82.4 ± 8.1	1	0.84	1.59
	Deposition density (kBq/m^2)			574		588		732			
H2	0–2	38	1.0	15500 ± 100	50	15900 ± 100	50	13800 ± 500	42	0.97	0.87
	2–4	35	0.9	13500 ± 100	39	13700 ± 100	39	13900 ± 600	38	0.99	1.01
	4–6	44	1.1	1570 ± 20	6	1590 ± 30	6	3690 ± 170	13	0.99	2.32
	6–10	68	0.9	679 ± 7	4	689 ± 10	4	909 ± 53	5	0.99	1.32
	10–15	112	1.1	88.3 ± 2.6	1	103 ± 4	1	199 ± 28	2	0.86	1.94
	15–20	97	1.0	117 ± 3	1	135 ± 4	1	ND		0.86	
	Deposition density (kBq/m^2)			611		625		642			
H3	0–2	42	1.1	18000 ± 100	79	18300 ± 100	79	18400 ± 700	69	0.98	1.01
	2–4	37	1.0	4360 ± 50	17	4290 ± 70	17	7380 ± 380	25	1.02	1.72
	4–6	50	1.3	492 ± 10	3	502 ± 14	3	904 ± 77	4	0.98	1.80
	6–10	82	1.0	161 ± 4	1	154 ± 5	1	264 ± 41	2	1.04	1.72
	10–15	134	1.4	16.1 ± 1.4	0	18.1 ± 1.9	0	ND		0.89	
	15–20	123	1.3	10.3 ± 0.6	0	12.7 ± 0.8	0	ND		0.81	
	Deposition density (kBq/m^2)			487		490		565			
H4	0–2	43	1.1	12500 ± 100	62	12600 ± 100	62	14700 ± 900	58	0.99	0.87
	2–4	42	1.1	6410 ± 60	31	6480 ± 90	31	7980 ± 630	30	0.99	1.02
	4–6	43	1.1	1140 ± 20	6	1200 ± 30	6	2400 ± 220	9	0.95	2.32
	6–10	84	1.1	124 ± 3	1	127 ± 5	1	370 ± 66	3	0.98	1.32
	10–15	117	1.2	11.6 ± 1.6	0	18.8 ± 2.1	0	ND		0.62	
	15–20	122	1.2	16.0 ± 0.8	0	19.9 ± 1.0	0	ND		0.80	
	Deposition density (kBq/m^2)			441		449		561			
Average	0–2		1.1 ± 0.1	15200 ± 3200	66 ± 16	15500 ± 3300	66 ± 16	15800 ± 2500	58 ± 12	0.98	0.97
	2–4		1.0 ± 0.2	6630 ± 4240	25 ± 12	6700 ± 4330	25 ± 12	9040 ± 3030	30 ± 6	0.99	1.59
	4–6		1.2 ± 0.1	1160 ± 710	5 ± 3	1180 ± 706	5 ± 3	2300 ± 1270	9 ± 4	0.97	2.07
	6–10		1.1 ± 0.1	358 ± 333	3 ± 2	371 ± 351	3 ± 2	479 ± 331	3 ± 2	0.97	1.37
	10–15		1.3 ± 0.1	61.7 ± 75.7	1 ± 1	70.1 ± 81.3	1 ± 1			0.81	
	15–20		1.3 ± 0.2	37.9 ± 46.6	0 ± 0	45.5 ± 52.9	0 ± 0			0.74	
	Deposition density (kBq/m^2)			512 ± 76		522 ± 80		608 ± 79			

H0 was sampled on April 23, 2011, the others were collected on April 24, 2011. Decay correction was made to April 1, 2011.
ND expresses not detected.

Table 2. Depth distribution of ^{134}Cs, ^{137}Cs, and ^{131}I concentrations in the orchard

	Depth (cm)	Weight (g)	Bulk density (g/cm^3)	^{134}Cs (Bq/kg dw)	Inventory (%)	^{137}Cs (Bq/kg dw)	Inventory (%)	^{131}I (Bq/kg dw)	Inventory (%)	^{134}Cs/^{137}Cs	^{131}I/^{137}Cs
K0	0–2	36	0.9	3650 ± 50	84	3620 ± 60	83	11000 ± 2400		1.01	3.04
	2–4	77	2.0	155 ± 8	8	189 ± 12	9	ND		0.82	
	4–6	73	1.9	117 ± 5	6	112 ± 7	5	ND		1.04	
	6–10	121	1.5	26.9 ± 1.7	2	31.3 ± 2.4	2	ND		0.86	
	10–15	142	1.5	3.6 ± 1.5	0	4.6 ± 1.0	0	ND		0.79	
	15–20	135	1.4	1.4 ± 0.3	0	1.4 ± 0.5	0	ND		1.01	
	Deposition density (kBq/m^2)			79		80		203			
K1	0–2	53	1.4	15400 ± 100	95	16000 ± 100	95	21300 ± 500	94	0.96	1.33
	2–4	48	1.2	357 ± 13	2	376 ± 20	2	1190 ± 100	4	0.95	3.17
	4–6	57	1.5	173 ± 6	1	188 ± 9	1	283 ± 38	1	0.92	1.50
	6–10	131	1.7	109 ± 3	2	111 ± 4	2	ND		0.98	
	10–15	133	1.4	26.4 ± 0.8	0	27.9 ± 1.1	0	31.7 ± 8.5	0	0.95	1.13
	15–20	150	1.5	6.8 ± 0.6	0	10.0 ± 0.7	0	ND		0.68	
	Deposition density (kBq/m^2)			440		459		616			
K2	0–2	48	1.2	14100 ± 100	92	14600 ± 100	92	20300 ± 1600	87	0.97	1.39
	2–4	63	1.6	501 ± 14	4	529 ± 21	4	1600 ± 360	9	0.95	3.03
	4–6	64	1.6	83.8 ± 3.1	1	87.0 ± 4.2	1	666 ± 212	4	0.96	7.65
	6–10	118	1.5	108 ± 3	2	110 ± 4	2	ND		0.98	
	10–15	144	1.5	22.7 ±1.6	0	20.1 ±1.9	0	ND		1.13	
	15–20	131	1.3	38.4 ± 1.0	1	41.3 ± 1.4	1	ND		0.93	
	Deposition density (kBq/m^2)			376		391		570			
K3	0–2	52	1.3	14500 ± 100	89	14900 ± 100	89	15600 ± 2800	73	0.97	1.05
	2–4	75	1.9	586 ± 15	5	605 ± 22	5	4040 ± 870	27	0.97	6.67
	4–6	72	1.8	482 ± 10	4	495 ± 14	4	ND		0.97	
	6–10	112	1.4	80.1 ± 2.8	1	94.7 ± 3.8	1	ND		0.85	
	10–15	145	1.5	9.9 ± 1.5	0	13.3 ± 1.6	0	ND		0.75	
	15–20	139	1.4	28.0 ± 0.8	0	30.5 ± 1.1	0	ND		0.92	
	Deposition density (kBq/m^2)			430		443		566			
K4	0–2	42	1.1	9990 ± 70	93	10200 ± 100	93	16500 ± 3100	90	0.98	1.62
	2–4	66	1.7	289 ± 13	4	298 ± 18	4	ND		0.97	
	4–6	66	1.7	42.9 ± 4.2	1	44.1 ± 5.0	1	1110 ± 380	10	0.97	25.1
	6–10	112	1.4	35.8 ± 2.9	1	40.8 ± 3.8	1	ND		0.88	
	10–15	144	1.5	32.8 ± 1.7	1	35.9 ± 2.4	1	ND		0.91	
	15–20	140	1.4	ND	0	2.0 ± 0.6	0	ND			
	Deposition density (kBq/m^2)			230		236		392			
Average	0–2		1.2 ± 0.2	11500 ± 4900	91 ± 4	11900 ± 5100	95 ± 5	16900 ± 4100		0.98	1.68
	2–4		1.7 ± 0.3	378 ± 170	5 ± 2	399 ± 169	5 ± 3	2280 ± 1540		0.93	4.29
	4–6		1.7 ± 0.2	180 ± 176	2 ± 2	185 ± 181	2 ± 2	686 ± 414		0.97	11.4
	6–10		1.5 ± 0.1	71.9 ± 38.9	1 ± 0	77.6 ± 38.6	2 ± 1			0.91	
	10–15		1.4 ± 0.1	19.1 ± 12.0	0 ± 0	20.3 ± 12.2	1 ± 0			0.91	
	15–20		1.4 ± 0.1	18.7 ± 17.5	0 ± 0	17.0 ± 18.0	0 ± 0			0.89	
	Deposition density (kBq/m^2)			311 ± 154		322 ± 161		469 ± 172			

K0 was sampled on April 23, 2011, the others were collected on April 24, 2011. Decay correction was made to April 1, 2011.
ND expresses not detected.

Table 3. Depth distribution of ^{134}Cs, ^{137}Cs, and ^{131}I concentrations in the rice paddy

	Depth (cm)	Weight (g)	Bulk density (g/cm^3)	^{134}Cs (Bq/kg dw)	Inventory (%)	^{137}Cs (Bq/kg dw)	Inventory (%)	^{131}I (Bq/kg dw)	Inventory (%)	^{134}Cs/^{137}Cs	^{131}I/^{137}Cs
S0	0–2	66	1.7	626 ± 7	88	652 ± 9	85	2710 ± 280		0.96	4.16
	2–4	81	2.1	35.0 ± 3.1	6	44.3 ± 4.4	7	ND		0.79	
	4–6	62	1.6	25.3 ± 4.2	3	30.2 ± 4.1	4	ND		0.84	
	6–10	124	1.6	6.8 ± 1.9	2	6.9 ± 1.7	2	ND		0.99	
	10–15	140	1.4	1.5 ± 0.6	0	6.0 ± 0.6	2	ND		0.25	
	15–20	134	1.4	2.6 ± 1.0	1	4.4 ± 0.6	1	ND		0.59	
	Deposition density (kBq/m^2)			24		26		92			
S1	0–2	49	1.2	4660 ± 70	97	4770 ± 100	96	10100 ± 500	94	0.98	2.12
	2–4	55	1.4	71.0 ± 6.3	2	86.0 ± 9.2	2	549 ± 84	6	0.83	6.39
	4–6	61	1.6	22.8 ± 3.0	1	21.0 ± 4.6	1	ND		1.09	
	6–10	101	1.3	5.6 ± 1.2	0	8.8 ± 1.7	0	ND		0.64	
	10–15	119	1.2	8.2 ± 0.5	0	12.7 ± 0.7	1	31.3 ± 5.7	1	0.64	2.46
	15–20	115	1.2	5.0 ± 0.8	0	11.7 ± 0.9	1	ND		0.43	
	Deposition density (kBq/m^2)			120		124		270			
S2	0–2	64	1.6	1470 ± 30	97	1450 ± 40	95	2760 ± 360		1.01	1.90
	2–4	56	1.4	29.3 ± 3.5	2	27.7 ± 4.6	2	ND		1.06	
	4–6	56	1.4	8.7 ± 2.3	1	15.7 ± 2.8	1	ND		0.55	
	6–10	95	1.2	3.1 ± 1.0	0	7.7 ± 1.5	1	ND		0.40	
	10–15	125	1.3	1.7 ± 0.6	0	5.7 ± 0.8	1	ND		0.30	
	15–20	112	1.1	6.2 ± 0.6	1	9.4 ± 0.7	1	ND		0.66	
	Deposition density (kBq/m^2)			50		50		90			
S3	0–2	68	1.7	2680 ± 30	97	2730 ± 50	97	8630 ± 850	94	0.98	3.16
	2–4	49	1.2	59.8 ± 4.6	2	51.8 ± 5.9	1	706 ± 182	6	1.16	13.6
	4–6	60	1.5	12.8 ± 1.7	0	18.5 ± 2.3	1	ND		0.69	
	6–10	144	1.8	6.6 ± 1.2	1	8.1 ± 1.0	1	ND		0.81	
	10–15	134	1.4	4.8 ± 0.6	0	7.6 ± 0.7	1	ND		0.63	
	15–20	111	1.1	3.1 ± 0.7	0	6.0 ± 0.7	0	ND		0.52	
	Deposition density (kBq/m^2)			95		97		315			
S4	0–2	43	1.1	26700 ± 100	66	27300 ± 200	66	25500 ± 1767	53	0.98	0.93
	2–4	46	1.2	12100 ± 100	32	12500 ± 100	32	21000 ± 1166	47	0.97	1.68
	4–6	40	1.0	281 ± 9	1	308 ± 14	1	ND		0.92	
	6–10	119	1.5	58.3 ± 2.3	0	61.3 ± 3.2	0	ND		0.95	
	10–15	119	1.2	57.9 ± 1.1	0	62.1 ± 1.5	0	ND		0.93	
	15–20	140	1.4	98.6 ± 1.3	1	102 ± 2	1	ND		0.97	
	Deposition density (kBq/m^2)			887		912		1050			
Average	0–2		1.5 ± 0.3	7230 ± 10990	89 ± 13	7380 ± 11240	88 ± 13	9940 ± 9320		0.98	2.45
	2–4		1.5 ± 0.4	2460 ± 5390	9 ± 13	2540 ± 5570	9 ± 13	7420 ± 11760		0.96	7.24
	4–6		1.4 ± 0.2	70.2 ± 118.3	1 ± 1	78.6 ± 128.1	1 ± 1			0.82	
	6–10		1.5 ± 0.2	16.1 ± 23.6	1 ± 1	18.5 ± 23.9	1 ± 1			0.76	
	10–15		1.3 ± 0.1	14.8 ± 24.3	0 ± 0	18.8 ± 24.3	1 ± 0			0.55	
	15–20		1.2 ± 0.1	23.1 ± 42.2	1 ± 0	26.7 ± 42.2	1 ± 0			0.63	
	Deposition density (kBq/m^2)			235 ± 366		242 ± 377		363 ± 397			

S0 was sampled on April 23, 2011, the others were collected on April 24, 2011. Decay correction was made to April 1, 2011.
ND expresses not detected.

Table 4. Depth distribution of ^{134}Cs, ^{137}Cs, and ^{131}I concentrations in the forest

	Depth (cm)	Weight (g)	Bulk density (g/cm^3)	^{134}Cs (Bq/kg dw)	Inventory (%)	^{137}Cs (Bq/kg dw)	Inventory (%)	^{131}I (Bq/kg dw)	Inventory (%)	^{134}Cs/^{137}Cs	^{131}I/^{137}
F0	Litter	1.3		190000 ± 1000	88	193000 ± 1000	88	ND		0.98	
	0–2	26	0.7	1260 ± 20	11	1250 ± 20	11	ND		1.01	
	2–4	44	1.1	29.9 ± 2.1	0	32.4 ± 2.6	0	ND		0.92	
	4–6	64	1.6	11.3 ± 1.4	0	19.6 ± 1.9	0	ND		0.58	
	6–10	98	1.2	6.6 ± 0.4	0	11.4 ± 0.5	0	ND		0.58	
	10–15	89	0.9	4.8 ± 0.6	0	8.6 ± 0.8	0	ND		0.55	
	Deposition density (kBq/m^2)			147		151					
F1	Litter	2.4		60800 ± 400	84	62200 ± 600	83	78600 ± 3400	59	0.98	1.2
	0–2	33	0.8	657 ± 21	13	684 ± 30	12	3350 ± 190	35	0.96	4.9
	2–4	37	1.0	75.6 ± 7.4	2	75.1 ± 10.1	2	409 ± 70	5	1.01	5.4
	4–6	49	1.3	6.9 ± 2.5	0	14.1 ± 2.4	0	ND		0.49	
	6–10	94	1.2	7.5 ± 0.7	0	16.0 ± 1.0	1	32.9 ± 6.0	1	0.47	2.0
	10–15	150	1.5	4.0 ± 0.6	0	11.7 ± 0.7	1	ND		0.34	
	Deposition density (kBq/m^2)			88		91		161			
F2	Litter	2.5		109000 ± 1000	74	109000 ± 1000	74	158000 ± 22000		1.00	1.4
	0–2	29	0.7	1720 ± 40	14	1670 ± 50	13	ND		1.03	
	2–4	40	1.0	936 ± 24	10	1000 ± 40	11	ND		0.94	
	4–6	50	1.3	58.5 ± 4.6	1	59.9 ± 6.2	1	ND		0.98	
	6–10	94	1.2	28.2 ± 1.9	1	35.2 ± 2.6	1	ND		0.80	
	10–15	109	1.1	13.3 ± 0.4	0	19.8 ± 0.6	0	ND		0.67	
	Deposition density (kBq/m^2)			183		185		197			
F3	Litter	2.6		123000 ± 1000	74	127000 ± 1000	75	ND		0.97	
	0–2	25	0.6	2200 ± 60	13	2090 ± 90	12	ND		1.05	
	2–4	46	1.2	845 ± 22	9	912 ± 32	9	ND		0.93	
	4–6	60	1.5	134 ± 6	2	131 ± 9	2	ND		1.03	
	6–10	111	1.4	29.5 ± 3.0	1	38.8 ± 4.1	1	ND		0.76	
	10–15	108	1.1	20.8 ± 0.6	1	27.0 ± 0.8	1	ND		0.77	
	Deposition density (kBq/m^2)			220		226					
F4	Litter	2.7		139000 ± 1000	86	141000 ± 1000	86	ND		0.99	
	0–2	24	0.6	2370 ± 70	13	2350 ± 100	12	ND		1.01	
	2–4	35	0.9	76.7 ± 3.8	1	89.2 ± 5.1	1	ND		0.86	
	4–6	41	1.1	24.0 ± 1.7	0	32.1 ± 2.4	0	ND		0.75	
	6–10	88	1.1	16.0 ± 2.8	0	22.0 ± 3.5	0	ND		0.73	
	10–15	110	1.1	10.2 ± 0.4	0	13.3 ± 0.6	0	ND		0.77	
	Deposition density (kBq/m^2)			224		226					
Average	Litter			124000 ± 47000	81 ± 7	126000 ± 48000	81 ± 6			0.98	
	0–2		0.7 ± 0.1	1640 ± 700	13 ± 1	1610 ± 670	12 ± 1			1.01	
	2–4		1.0 ± 0.1	393 ± 456	4 ± 5	424 ± 489	5 ± 5			0.93	
	4–6		1.3 ± 0.2	47.0 ± 52.9	1 ± 1	51.4 ± 48.0	1 ± 1			0.76	
	6–10		1.2 ± 0.1	17.6 ± 10.9	0 ± 0	24.7 ± 11.9	1 ± 0			0.67	
	10–15		1.2 ± 0.2	10.6 ± 6.9	0 ± 0	16.1 ± 7.3	0 ± 0			0.62	
	Deposition density (kBq/m^2)			172 ± 57		176 ± 57		179 ± 25			

F0 was sampled on April 23, 2011, the others were collected on April 24, 2011. Decay correction was made to April 1, 2011.
ND expresses not detected.

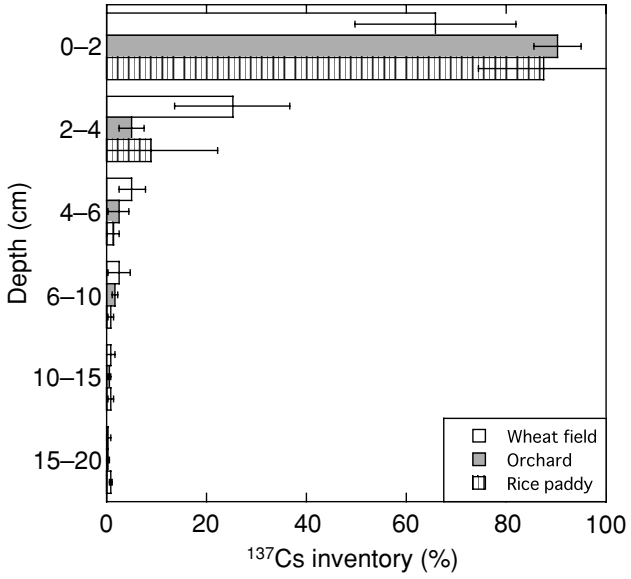

Fig. 1. Depth profiles of the inventories of ^{137}Cs in the various agricultural fields. The inventories are expressed as a percentage of the total inventory. The error bars represent the standard deviation from 5 samples.

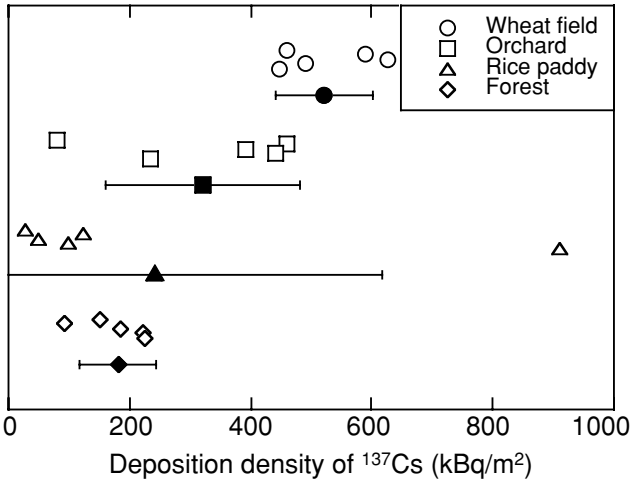

Fig. 2. Deposition densities of ^{137}Cs in the different agricultural fields and the forest. The solid symbols are the mean of the 5 sample sets, and the open symbols represent each sample set. The error bars represent the standard deviation from 5 samples.

radiocesium within 2 cm of the surface varied from 83% to 95%. These depth-profile results demonstrate that more than 90% of the ^{134}Cs, ^{137}Cs, and ^{131}I were distributed within 4 cm of the soil surface. The total activities (the sum over the entire depth) of ^{134}Cs, ^{137}Cs, and ^{131}I in the orchard were in the ranges 156–865, 160–900, and 398–1210 Bq, respectively, and the deposition densities of ^{134}Cs, ^{137}Cs, and ^{131}I were estimated to be 311 ± 155 (SD, n = 5), 322 ± 161 (SD, n = 5), and 469 ± 172 (SD, n = 5) kBq/m^2, respectively.

The concentrations of ^{134}Cs, ^{137}Cs, and ^{131}I in the rice paddy are shown in Table 3. As in the case of the orchard, the radioactivity of ^{131}I was not detected in many samples. The radiocesium concentrations within 2 cm of the surface varied widely; they were in the range 626–26700 Bq/kg on a dry weight basis. The difference between the minimum and maximum values was almost two orders of magnitude. This large variation for the rice paddy can be explained as follows. At the time of the accident, rice fields in this area were not covered with water. When the radioactivity-containing rain fell on the rice field, it left puddles on the field because of the bad drainage of the paddy soil. This likely resulted in the heterogeneous distribution of radionuclides observed in the rice field. The radiocesium concentrations within 2 cm of the surface varied from 66% to 97%. The results of the depth profiles demonstrate that more than 90% of the ^{134}Cs and ^{137}Cs were distributed within 4 cm of the soil surface. This result is consistent with a previous study (Shiozawa *et al.*, 2011). The total activities of ^{134}Cs, ^{137}Cs, and ^{131}I in the rice paddy were in the ranges 50–1740, 50–1790, and 180–2060 Bq, respectively, and the deposition densities of ^{134}Cs, ^{137}Cs, and ^{131}I were calculated to be 235 ± 367 (SD, n = 5), 242 ± 376 (SD, n = 5), and 363 ± 397 (SD, n = 5) kBq/m^2, respectively.

Figure 1 shows the inventories of ^{137}Cs in the various agricultural fields. The degree of penetration of ^{137}Cs in the wheat field was larger than that in the orchard, which could be caused by the higher porosity of the soil in the wheat field. This feature of the wheat field results in smaller variability of the deposition densities (Fig. 2). On the contrary, the low permeability of the orchard and paddy soils may cause horizontal migration of radionuclides during initial deposition, which might result in smaller amounts of deposition densities and larger variations in the radionuclide concentrations. For that reason, we believe that the deposition densities for the wheat field (^{134}Cs, 512 ± 76; ^{137}Cs, 522 ± 80; ^{131}I, 608 ± 79 kBq/m^2) are appropriate for estimating the amount of fallout in this area.

Sutherland (1996) recommended a total of 11 soil core samples for reliable estimation of the local inventory. The small numbers of soil samples in this study might cause a biased estimation. Therefore, we calculated the deposition density from the 15 core samples collected in the three adjacent agricultural fields, and the mean deposition densities of ^{134}Cs, ^{137}Cs, and ^{131}I were calculated to be 353 ± 248 (SD, n = 15; range: 24–887), 362 ± 254 (SD, n = 15; range: 26–912), and 468 ± 275 (SD, n = 12; range: 92–1050) kBq/m^2, respectively. The map of the

radioactive cesium concentration in the soil by MEXT indicates that the ^{137}Cs inventory for the study site was 323 kBq/m^2 and those within a radius of 4 km of the study site were in the range 24–513 kBq/m^2 (decay corrected to April 1, 2011), which is compatible with our observation. However, the amount of ^{137}Cs inventory estimated by the MEXT airborne monitoring survey (^{137}Cs, 100–300 kBq/m^2) is smaller than that of our results. We think this inconsistency could be caused by the limited resolution of the airborne monitoring survey.

Depth profiles of ^{134}Cs, ^{137}Cs, and ^{131}I in the cedar forest are shown in Table 4. The radioactivities of ^{131}I in most of the forest samples were below the limit of detection owing to its short half-life, and therefore, a single depth profile for ^{131}I might not be sufficient to characterize the total ^{131}I fallout in the cedar forest. A high proportion of radiocesium in the leaf litter samples (74% to 88%) was observed. The depth-profile results demonstrate that more than 90% of ^{134}Cs, ^{137}Cs, and ^{131}I were distributed within 4 cm of the surface (including litter). The total activities of ^{134}Cs, ^{137}Cs, and ^{131}I for the core samples including the litter were calculated to be 172–439, 180–444, and 316–386 Bq, respectively, and the deposition densities of ^{134}Cs, ^{137}Cs, and ^{131}I were estimated to be 172 ± 57 (SD, n = 5), 176 ± 56 (SD, n = 5), and 179 ± 25 (SD, n = 2) kBq/m^2, respectively. In the cedar forest, the deposition density of radiocesium showed little variation when compared to that of the orchard and rice paddy (Fig. 2). It is interesting to note that the deposition density in the cedar forest was less than half that of the wheat field. This indicates that a certain amount of radioactive fallout still remains on the tree canopies. Assuming the deposition level observed in the wheat field is representative for this area, more than half of the fallout landing on evergreen forestland is still distributed in the tree canopies.

The ratio of ^{134}Cs/^{137}Cs was calculated in the surface layers (0–2 cm or litter) that showed the highest radioactivity concentrations. The mean ratios (decay corrected to April 1) for each surface layer in the wheat field, orchard, rice paddy, and forest are 0.981, 0.975, 0.982, and 0.983, respectively. The average ^{134}Cs/^{137}Cs ratio for these 4 values is 0.980 ± 0.004, which agrees with the reported data (MEXT, 2011). Significant changes in the ratio with depth were observed for samples with lower concentrations of radiocesium, suggesting contributions of ^{137}Cs from nuclear weapons fallout (NIAES, 2010).

The ratio of ^{131}I/^{137}Cs was also calculated, although ^{131}I was not detected in some samples, as mentioned previously. The ratio of ^{131}I/^{137}Cs tended to increase with depth, suggesting that the deposited radioiodine migrated into deeper soil layers faster than radiocesium. Tanaka *et al*. (2012) carried out leaching experiments using contaminated soil samples collected in Fukushima. They reported that iodine was more extractable than cesium and mainly in organic form. Previous studies showed that cesium was strongly adsorbed onto clay minerals (Tsukada *et al*., 2008). These characteristics are consistent with the fact that radioiodine is more readily distributed to deeper layers. For the surface soil samples (0–2 cm), the ratio of ^{131}I/^{137}Cs was in the range 1.0–4.2 (decay corrected to April 1, 2011) and tended to increase with decreasing concentrations of radionuclides, suggesting post-depositional migration.

Conclusion

We investigated the depth distributions of ^{134}Cs, ^{137}Cs, and ^{131}I in three different types of agricultural fields and a cedar forest. Our results demonstrate that more than 90% of the radionuclides were distributed within 6 cm of the surface at the wheat field and within 4 cm of the surface at the rice paddy, orchard, and cedar forest. Large variations in the concentrations of radiocesium and radioiodine within the rice paddy were observed. We hypothesize that rain containing radioactive fallout initially formed puddles in the rice field resulting in the presently observed heterogeneities in the distribution of radionuclides. In comparing profiles of radioiodine and radiocesium and their ratios in the different agricultural plots, we observed faster vertical migration of radioiodine than radiocesium.

Because of the smaller dispersion and higher radioactivity, the deposition density of the wheat field is appropriate for an estimate of the overall amount of fallout in this area. Comparison of the deposition density between the wheat field and the cedar forest suggests that more than half of the radioactive fallout that has landed on evergreen forestland still remains in the tree canopies.

Acknowledgments—We are grateful to Drs. T. Ohtsuki and H. Kikunaga (Tohoku Univ.) for constructive comments. We thank Ms. M. Arai for the sample preparation. We thank Dr. G. Snyder (Rice University) for the critical reading of the manuscript. We are also grateful to two anonymous reviewers and Prof. Y. Takahashi (Hiroshima Univ.) for their constructive comments. This study was supported in part by a grant from the Strategic Research Foundation Grant-aided Project from the Ministry of Education, Culture, Sport, Science, and Technology, Japan (MEXT).

References

Almgren, S. and Isaksson, M. (2006) Vertical migration studies of ^{137}Cs from nuclear weapons fallout and the Chernobyl accident. *J. Environ. Radioact*. **91**, 90–102.

Beck, H. L. (1966) Environmental gamma radiation from deposited fission products, 1960–1964. *Health Phys*. **12**, 313–322.

Bunzl, K., Schimmack, W., Krouglov, S. V. and Alexakhin, R. M. (1995) Changes with time in the migration of radiocaesium in the soil, as observed near Chernobyl and

in Germany, 1986–1994. *Sci. Total Environ.* **175**, 49–56.

Chino, M., Nakayama, H., Nagai, H., Terada, H., Katata, G. and Yamazawa, H. (2011) Preliminary Estimation of Release Amounts of ^{131}I and ^{137}Cs Accidentally Discharged from the Fukushima Daiichi Nuclear Power Plant into the Atmosphere. *J. Nucl. Sci. Tech.* **48**, 1129–1134.

Ivanov, Y. A., Lewyckyj, N., Levchuk, S. E., Prister, B. S., Firsakova, S. K., Arkhipov, N. P., Arkhipov, A. N., Kruglov, S. V., Alexakhin, R. M., Sandalls, J. and Askbrant, S. (1997) Migration of ^{137}Cs and ^{90}Sr from Chernobyl Fallout in Ukrainian, Belarussian and Russian Soils. *J. Environ. Radioact.* **35**, 1–21.

Kato, H., Onda, Y. and Teramage, M. (2012) Depth distribution of ^{137}Cs, ^{134}Cs, and ^{131}I in soil profile after Fukushima Dai-ichi Nuclear Power Plant Accident. *J. Environ. Radioact.* **111** (in press).

Kinoshita, N., Suekia, K., Sasa, K., Kitagawa, J., Ikarashi, S., Nishimura, T., Wong, Y.-S., Satou, Y., Handa, K., Takahashi, T., Sato, M. and Yamagata, T. (2011) Assessment of individual radionuclide distributions from the Fukushima nuclear accident covering central-east Japan. *PNAS* **108**, 19526–19529.

Ministry of Education, Culture, Sports, Science and Technology, Japan (MEXT) (2011) Monitoring information of environmental radioactivity level. Available at http://radioactivity.mext.go.jp/en/

Muramatsu, Y., Sumiya, M. and Ohmomo, Y. (1987) Iodine-131 and other radionuclides in environmental samples collected from Ibaraki/Japan after the Chernobyl accident. *Sci. Total Environ.* **67**, 149–158.

National Institute for Agro-Environmental Sciences (NIAES) (2010) Database on ^{90}Sr and ^{137}Cs of the Main Cereals and Agricultural Soils. Available at http://psv92.niaes3.affrc.go.jp/vgai_agrip/samples

Orlov, M. Y., Snykov, V. P., Khvalenskii, Y. A. and Volokitin, A. A. (1996) Contamination of the soil of the European part of the territory of the USSR with ^{131}I after the Chernobyl nuclear accident. *At. Energ.* **80**, 439–444.

Qin, H., Yokoyama, Y., Fan, Q., Iwatani, H., Tanaka, K., Sakaguchi, A., Kanai, Y., Zhu, J., Onda, Y. and Takahashi, Y. (2012) Investigation of cesium adsorption on soil and sediment samples from Fukushima Prefecture by sequential extraction and EXAFS technique. *Geochem. J.* **46**, this issue, 297–302.

Rosén, K., Öborn, I. and Lönsjö, H. (1999) Migration of radiocaesium in Swedish soil profiles after the Chernobyl accident, 1987–1995. *J. Environ. Radioact.* **46**, 45–66.

Shiozawa, S., Tanoi, K., Nemoto, K., Yoshida, S., Nishida, K., Hashimoto, K., Sakurai, K., Nakanishi, T. M., Nihei, N. and Ono, Y. (2011) Vertical concentration profiles of radioactive caesium and convective velocity in soil in a paddy field in Fukushima. *Radioisotopes* **60**, 323–328.

Sutherland, R. A. (1996) Caesium-137 soil sampling and inventory variability in reference locations: a literature review. *Hydrol. Process* **10**, 43–53.

Tanaka, K., Takahashi, Y., Sakaguchi, A., Umeo, M., Hayakawa, S., Tanida, H., Saito, T. and Kanai, Y. (2012) Vertical profiles of Iodine-131 and Cesium-137 in soils in Fukushima Prefecture related to the Fukushima Daiichi Nuclear Power Station Accident. *Geochem. J.* **46**, 73–76.

Tsukada, H., Takeda, A., Hisamatsu, S. and Inaba, J. (2008) Concentration and specific activity of fallout ^{137}Cs in extracted and particle-size fractions of cultivated soils. *J. Environ. Radioact.* **99**, 875–881.

Watanabe, T., Tsuchiya, N., Oura, Y., Ebihara, M., Inoue, C., Hirano, N., Yamada, R., Yamasaki, S., Okamoto, A., Watanabe Nara, F. and Nunohara, K. (2012) Distribution of artificial radionuclides (^{110m}Ag, ^{129m}Te, ^{134}Cs, ^{137}Cs) in surface soils from Miyagi Prefecture, northeast Japan, following the 2011 Fukushima Dai-ichi nuclear power plant accident. *Geochem. J.* **46**, this issue, 279–285.